IOP Publishing New J. Phys. 26 (2024) 063015 https://doi.org/10.1088/1367-2630/ad503e

New Journal of Physics
The open access journal at the forefront of physics

Deutsche Physikalische Gesellschaft DPG
IOP Institute of Physics

Published in partnership with: Deutsche Physikalische Gesellschaft and the Institute of Physics

OPEN ACCESS

RECEIVED
20 March 2024

REVISED
21 May 2024

ACCEPTED FOR PUBLICATION
24 May 2024

PUBLISHED
11 June 2024

PAPER

Lattice polaron in a Bose–Einstein condensate of hard-core bosons

Moroni Santiago-García[1], **Shunashi G Castillo-López**[2] **and Arturo Camacho-Guardian**[2,*]

[1] Instituto Nacional de Astrofísica, Óptica y Electrónica, Calle Luis Enrique Erro No.1 Santa María Tonantzintla, Puebla, CP 72840, Mexico
[2] Instituto de Física, Universidad Nacional Autónoma de México, Apartado Postal 20-364, Ciudad de México, CP 01000, Mexico
[*] Author to whom any correspondence should be addressed.

E-mail: acamacho@fisica.unam.mx

Keywords: polaron, optical lattices, Holstein-Primakoff, quasiparticles

Abstract

Lattice polarons, quasiparticles arising from the interaction between an impurity and its surrounding bosonic environment confined to a lattice system, have emerged as a platform for generating complex few-body states, probing many-body phenomena, and addressing long-standing problems in physics. In this study, we employ a variational ansatz to investigate the quasiparticle and spectral properties of an impurity coupled to a condensate gas of hard-core bosons in a two-dimensional optical lattice. Our findings demonstrate that the polaron features can be tuned by adjusting the filling factor of the bath, revealing intriguing polaron characteristics in the strongly interacting regime. These results offer valuable insights for lattice polaron experiments with ultracold gases and can serve as a guide for new experiments in emergent quantum devices, such as moiré materials, where optical excitations can be described in terms of hard-core bosons.

1. Introduction

Ultracold gases have served as a robust platform for quantum simulation of exotic many-body physics [1–4]. This permitted the realization of quantum analogs of well-understood phenomena [5, 6], as well as the exploration of physics beyond the accessible regimes in condensed matter physics. Nowadays, the versatility of these systems allows for addressing concise proposals for long-standing open problems such as high-temperature superconductivity. Bose polaron physics in ultracold gases has attracted much attention given this context, and it has dramatically stimulated new theoretical and numerical approaches [7–31] to understanding the experimental realization of this phenomenon far beyond its original formulation [32–39].

In optical lattices, impurity physics has renewed interest in probing the Mott-insulator to superfluid transition [40], topological phases [41–43], band geometry [44], magnetic polarons [45–49], few-body physics [50], non-equilibrium dynamics [51], and polaron physics in strongly correlated Fermi–Hubbard models [52]. The study of lattice polarons is further motivated by the advances in quantum gas microscopy, which enables the imaging of individual atoms [53, 54], providing intricate spatial details of quantum states that complement traditional spectroscopic information [45, 55].

In condensed matter systems, recent experiments with cavity-coupled monolayer semiconductors have reported the realization of the first strongly interacting two-dimensional polarons in the context of polaron-polaritons [56–59]. The underlying character of these quasiparticles has unveiled new questions to understand polaron physics for open systems [60, 61], photon bound states [62, 63], and few-body states of polaritons [64]. Furthermore, the recent developments with two-dimensional van der Waals heterostructures place quantum gases into new territories where polaron physics and Bose–Fermi mixtures are being realized with control and tunability [65] with excitons and charge carriers (electrons and holes). Polaron physics has demonstrated to be a powerful tool to sense correlated phases of matter [66–70]. In these experiments, Bose–Fermi Hubbard systems may arise as a consequence of an emergent moiré potential [71–73]. In multilayers, spatially indirect excitons (electron and hole sitting in different layers) can arise, imprinting

strong dipole–dipole interactions, which can effectively lead to a Hubbard model sensitive to the intrinsic quasi-bosonic character of the excitations [74]. Indeed, for relevant experiments, the excitons in a moiré superlattice may behave as hard-core bosons, which have been predicted to exhibit superfluid [75] and supersolid phases [76].

Motivated by the progress with ultracold gases and the relevance in the new quantum materials, in this article, we study the strongly interacting impurity in a Bose–Einstein condensate (BEC) of hard-core bosons in the atomic context. For this purpose, we employ a variational ansatz to describe the spectral and quasiparticle properties of an impurity embedded in a gas of hard-core bosons. The character of the variational ansatz allows us to understand the coupling between the collective excitations of the hard-core gas and the impurity beyond the so-called Fröhlich-like Hamiltonian, which is only valid for weak impurity-boson interactions. Our results show that the quasiparticle properties and the emergence of the polaron branches can be tuned with the underlying properties of the bath and find that for low densities, the quasiparticle properties are governed by the beyond Fröhlich Hamiltonian.

Our study is motivated and inspired by state-of-the-art experiments and the growing theoretical interest in quantum gases, where interactions between different species of atoms can be tuned on demand. In particular, in view of the experimental progress with Bose–Fermi and Bose–Bose Hubbard models [77–80], and in van der Waals heterostructures, where moiré excitons and electrons can be tightly confined to a moiré superlattice and highly imbalanced-population Bose–Fermi mixtures can be created to realize polaron physics [71–73]. Our theoretical framework may provide valuable guidance for understanding these experimental systems.

2. Model

We consider a single impurity coupled to an atomic ultracold two-dimensional gas of hard-core bosons confined in a square optical lattice of N_s sites, as illustrated in figure 1(b). The Hamiltonian of the system consists of three terms:

$$\hat{H} = \hat{H}_{\rm B} + \hat{H}_{\rm A} + \hat{H}_{\rm AB}. \tag{1}$$

The first term $\hat{H}_{\rm B}$ describes the gas of hard-core bosons, the second term $\hat{H}_{\rm A}$ represents the non-interacting Hamiltonian for the single impurity, and finally, $\hat{H}_{\rm AB}$ accounts for the impurity-boson coupling. To make our manuscript self-contained, we discuss each term separately in detail.

2.1. Collective excitations of a hard-core gas

We start describing the gas of hard-core bosons. The derivation outlined in this subsection can be found in [81, 82], however, to make our manuscript more pedagogical, we include here a detailed derivation.

The Hamiltonian of the majority bosons is given by

$$\hat{H}_{\rm B} = \sum_{\langle \mathbf{r},\mathbf{r}'\rangle} \left[-t_{\rm B} \left(\hat{c}^{\dagger}_{\mathbf{r},{\rm B}} \hat{c}_{\mathbf{r}',{\rm B}} + {\rm h.c.} \right) - \delta_{\mathbf{r},\mathbf{r}'} \mu_{\rm B} \hat{n}_{\mathbf{r},{\rm B}} \right] \tag{2}$$

$$+ \frac{U_{\rm BB}}{2} \sum_{\mathbf{r}} \hat{c}^{\dagger}_{\mathbf{r},{\rm B}} \hat{c}^{\dagger}_{\mathbf{r},{\rm B}} \hat{c}_{\mathbf{r},{\rm B}} \hat{c}_{\mathbf{r},{\rm B}}, \tag{3}$$

where the creation (annihilation) operator of the B atoms is denoted by $\hat{c}^{\dagger}_{\mathbf{r},{\rm B}}$ ($\hat{c}_{\mathbf{r},{\rm B}}$). The tunneling coefficients is given by $t_{\rm B}$, with a chemical potential of $\mu_{\rm B}$. We consider an on-site boson–boson interaction, $U_{\rm BB}$, much larger than the tunneling, $t_{\rm B}$, so we assume that the B atoms can effectively be regarded as hard-core bosons. Finally, $\hat{n}_{\mathbf{r},{\rm B}} = \hat{c}^{\dagger}_{\mathbf{r},{\rm B}} \hat{c}_{\mathbf{r},{\rm B}}$ corresponds to the number operator.

The idea is to account for the forbidden double occupancy of the B atoms. Then, we map the bosonic field operators into spin 1/2 operators; that is, replacing $\hat{c}^{\dagger}_{\mathbf{r},{\rm B}} \to \hat{S}^{\dagger}_{\mathbf{r}}$, and $\hat{c}_{\mathbf{r},{\rm B}} \to \hat{S}_{\mathbf{r}}$, where $\hat{S}^{\dagger}_{\mathbf{r}}$ ($\hat{S}_{\mathbf{r}}$) creates (annihilates) a spin $+\frac{1}{2}$ ($-\frac{1}{2}$) at location $\mathbf{r}$. Therefore, the Hamiltonian $\hat{H}_{\rm B}$ maps to

$$\hat{H}_{\rm B} = -t_{\rm B} \sum_{\langle \mathbf{r},\mathbf{r}'\rangle} \left(\hat{S}^{\dagger}_{\mathbf{r}} \hat{S}_{\mathbf{r}'} + {\rm h.c} \right) - \mu_{\rm B} \sum_{\mathbf{r}} \hat{S}^{z}_{\mathbf{r}} - \frac{\mu_{\rm B}}{2} N_s. \tag{4}$$

The ground state of the B atoms is written as

$$|\psi(\theta)\rangle_{\rm BEC} = \prod_{\mathbf{r}} \left[\sin\left(\frac{\theta}{2}\right) + \cos\left(\frac{\theta}{2}\right) \hat{S}^{\dagger}_{\mathbf{r}} \right] |0\rangle, \tag{5}$$

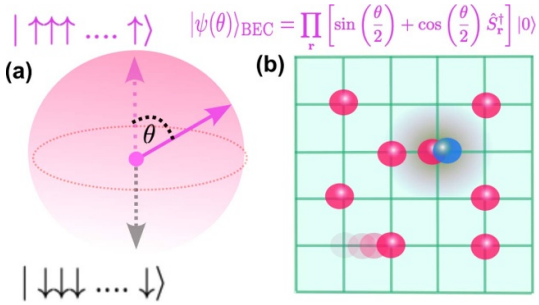

Figure 1. (a) Schematic representation of the state describing a Bose–Einstein condensate (BEC) of hard-core bosons in terms of the Bloch sphere, the angle θ determines the filling factor of the BEC. (b) Cartoon of the impurity (blue ball) coupled to the BEC of hard-core bosons (pink balls).

the many-body wave function consisting of N_s identical sites. Since we consider hard-core bosons, this many-body state can be understood in terms of the Bloch sphere as illustrated in figure 1(a). Here, the angle θ is determined by a variational approach [81]

$$\delta \frac{{}_{\rm BEC}\langle\psi(\theta)|\hat{H}_{\rm B}|\psi(\theta)\rangle_{\rm BEC}}{\delta\theta} = 0. \tag{6}$$

By minimizing the energy, we obtain a relation between the chemical potential and the angle θ: $\cos\theta = \mu_{\rm B}/4t_{\rm B}$, which defines the filling factor $n_{\rm B} = (\cos\theta + 1)/2$. The state of the system corresponds to a BEC with a condensate fraction of $n_0 = n_{\rm B}(1 - n_{\rm B})$ [81]. Interestingly, for non-local interactions, the phase-diagram is predicted to exhibit density-waves, superfluid, and supersolid phases [83]. The study of these exotic phases, is however, beyond the scope of our manuscript.

To arrive at our final Hamiltonian $\hat{H}_{\rm B}$, we perform three more transformations. First, we rotate our system about the y axis to align the z axis with the mean-field solution:

$$\begin{aligned}
\hat{S}^{x}_{\mathbf{r}} &= \cos\theta\hat{L}^{x}_{\mathbf{r}} + \sin\theta\hat{L}^{z}_{\mathbf{r}},\\
\hat{S}^{y}_{\mathbf{r}} &= \hat{L}^{y}_{\mathbf{r}},\\
\hat{S}^{z}_{\mathbf{r}} &= -\sin\theta\hat{L}^{x}_{\mathbf{r}} + \cos\theta\hat{L}^{z}_{\mathbf{r}}.
\end{aligned} \tag{7}$$

Second, we use the Holstein–Primakoff transformation, retaining the linear terms [84]

$$\begin{aligned}
\hat{L}^{x}_{\mathbf{r}} &= \frac{1}{2}\left(\hat{d}^{\dagger}_{\mathbf{r}} + \hat{d}_{\mathbf{r}}\right),\\
\hat{L}^{y}_{\mathbf{r}} &= \frac{1}{2i}\left(\hat{d}^{\dagger}_{\mathbf{r}} - \hat{d}_{\mathbf{r}}\right),\\
\hat{L}^{z}_{\mathbf{r}} &= \frac{1}{2} - \hat{d}^{\dagger}_{\mathbf{r}}\hat{d}_{\mathbf{r}},
\end{aligned} \tag{8}$$

where $\hat{d}^{\dagger}_{\mathbf{r}}, \hat{d}_{\mathbf{r}}$ are bosonic operators. In momentum space, the Hamiltonian can be written as

$$\hat{H}_{\rm B} \approx \sum_{\mathbf{k}} \alpha_{\mathbf{k}}\left(\hat{d}^{\dagger}_{\mathbf{k}}\hat{d}_{\mathbf{k}} + \hat{d}^{\dagger}_{-\mathbf{k}}\hat{d}_{-\mathbf{k}}\right) + \beta_{\mathbf{k}}\left(\hat{d}^{\dagger}_{\mathbf{k}}\hat{d}^{\dagger}_{-\mathbf{k}} + \hat{d}_{-\mathbf{k}}\hat{d}_{\mathbf{k}}\right), \tag{9}$$

with

$$\alpha_{\mathbf{k}} = \frac{1}{2}\left[\frac{\epsilon_{\mathbf{k}}}{2}\left(\cos^2\theta + 1\right) + 4t_{\rm B}\right], \tag{10a}$$

$$\beta_{\mathbf{k}} = -\frac{1}{4}\sin^2\theta\epsilon_{\mathbf{k}}. \tag{10b}$$

Here, $\epsilon_{\mathbf{k}} = -2t_{\rm B}[\cos(k_x a) + \cos(k_y a)]$, and a is the lattice constant.

To diagonalize Hamiltonian (9), we use a third and final transformation, in turn, the following Bogoliubov transformation,

$$\begin{aligned}
\hat{d}_{\mathbf{k}} &= u_{\mathbf{k}}\hat{\gamma}_{\mathbf{k}} - v_{\mathbf{k}}\hat{\gamma}^{\dagger}_{-\mathbf{k}}\\
\hat{d}^{\dagger}_{-\mathbf{k}} &= u_{\mathbf{k}}\hat{\gamma}^{\dagger}_{-\mathbf{k}} - v_{\mathbf{k}}\hat{\gamma}_{\mathbf{k}},
\end{aligned} \tag{11}$$

where the coherence factors of the BEC, $u_{\mathbf{k}}$ and $v_{\mathbf{k}}$ are defined as

$$u_{\mathbf{k}} = \sqrt{\frac{1}{2} + \frac{\alpha_{\mathbf{k}}}{2\sqrt{\alpha_{\mathbf{k}}^2 - \beta_{\mathbf{k}}^2}}}, \tag{12a}$$

$$v_{\mathbf{k}} = \sqrt{-\frac{1}{2} + \frac{\alpha_{\mathbf{k}}}{2\sqrt{\alpha_{\mathbf{k}}^2 - \beta_{\mathbf{k}}^2}}}. \tag{12b}$$

We finally arrive to the Hamiltonian $\hat{H}_{\mathrm{B}}$ written in terms of the collective excitations of the system, coined spin-waves [81]

$$\hat{H}_{\mathrm{B}} = \sum_{\mathbf{k}} \omega(\mathbf{k})\, \hat{\gamma}_{\mathbf{k}}^{\dagger} \hat{\gamma}_{\mathbf{k}}, \tag{13}$$

where $\hat{\gamma}_{\mathbf{k}}^{\dagger}$ and $\hat{\gamma}_{\mathbf{k}}$ are the creation and annihilation bosonic operators describing the collective excitations of the BEC, respectively, with $\omega(\mathbf{k}) = 2\sqrt{\alpha_{\mathbf{k}}^2 - \beta_{\mathbf{k}}^2}$. The dispersion of the collective excitations is linear at small momenta $\omega(\mathbf{k}) \sim c_s|\mathbf{k}|$, where the speed of sound c_s is given by $c_s = 2t\sqrt{1-\cos^2\theta}$. An extended discussion of the remaining BEC features such as the superfluid density, finite temperature effects, among others, lie beyond the scope of the manuscript, which, however, can be found in [81].

2.2. Impurity-Boson coupling

To describe the coupling between the impurity and the collective excitations of the BEC, we now turn our attention into the following terms of the Hamiltonian

$$\begin{aligned} \hat{H}_{\mathrm{A}} &= -t_{\mathrm{A}} \sum_{\langle \mathbf{r},\mathbf{r}' \rangle} \left(\hat{c}_{\mathbf{r},A}^{\dagger} \hat{c}_{\mathbf{r}',\mathrm{A}} + \mathrm{h.c.} \right), \\ \hat{H}_{\mathrm{AB}} &= U_{\mathrm{AB}} \sum_{\mathbf{r}} \hat{n}_{\mathbf{r},\mathrm{B}} \hat{n}_{\mathbf{r},\mathrm{A}}. \end{aligned} \tag{14}$$

The first line corresponds to $\hat{H}_{\mathrm{A}}$, which simply describes the hopping term with tunneling constant t_{A}. Here, $\hat{c}_{\mathbf{r},\mathrm{A}}^{\dagger}$ ($\hat{c}_{\mathbf{r},\mathrm{A}}$) denotes the creation (annihilation) operation of the impurity. The second line give $\hat{H}_{\mathrm{AB}}$ written in terms of the B atoms. Therefore, we perform the same transformations described above to the bosons operators, which allow us to write the impurity-boson term of the Hamiltonian $\hat{H}_{\mathrm{AB}}$ in terms of the coupling of the impurity to the collective excitations of the Bose gas as following

$$\begin{aligned} \hat{H}_{\mathrm{AB}} = {} & \frac{U_{\mathrm{AB}}}{2}(1+\cos\theta) \sum_{\mathbf{r}} \hat{n}_{\mathbf{r},A} \\ & - \frac{U_{\mathrm{AB}}}{\sqrt{N_s}} \frac{\sin\theta}{2} \sum_{\mathbf{k},\mathbf{q}} \left(u_{\mathbf{q}} - v_{\mathbf{q}}\right) \left(\hat{\gamma}_{-\mathbf{q}}^{\dagger} + \hat{\gamma}_{\mathbf{q}}\right) \hat{c}_{\mathbf{k}+\mathbf{q},A}^{\dagger} \hat{c}_{\mathbf{k},A} \\ & - \frac{1}{N_s} U_{\mathrm{AB}} \cos\theta \sum_{\mathbf{k},\mathbf{q},\mathbf{k}'} \left[u_{\mathbf{k}'+\mathbf{q}} u_{\mathbf{k}'} \hat{\gamma}_{\mathbf{k}'+\mathbf{q}}^{\dagger} \hat{\gamma}_{\mathbf{k}'} \right. \\ & - u_{\mathbf{k}'+\mathbf{q}} v_{\mathbf{k}'} \hat{\gamma}_{\mathbf{k}'+\mathbf{q}}^{\dagger} \hat{\gamma}_{-\mathbf{k}'}^{\dagger} - v_{\mathbf{k}'+\mathbf{q}} u_{\mathbf{k}'} \hat{\gamma}_{-(\mathbf{k}'+\mathbf{q})} \hat{\gamma}_{\mathbf{k}'} \\ & \left. + v_{\mathbf{k}'+\mathbf{q}} v_{\mathbf{k}'} \hat{\gamma}_{-(\mathbf{k}'+\mathbf{q})} \hat{\gamma}_{-\mathbf{k}'}^{\dagger} \right] \hat{c}_{\mathbf{k}-\mathbf{q},A}^{\dagger} \hat{c}_{\mathbf{k},A}. \end{aligned} \tag{15}$$

The impurity-boson Hamiltonian of equation (15) consists of three contributions: i) the mean-field term in the first line, ii) the Fröhlich-like interaction where a single collective excitation can be either absorbed or emitted (second line), and iii) beyond Fröhlich contributions (third to fifth lines), which involve processes with two collective modes. Notice that for $\theta \to \pi$, the interaction Hamiltonian is completely governed by the beyond Fröhlich term.

In summary, the Hamiltonian of the system is the sum of the following terms:

$$\hat{H} = \sum_{\mathbf{k}} \left[\omega(\mathbf{k})\, \hat{\gamma}_{\mathbf{k}}^{\dagger} \hat{\gamma}_{\mathbf{k}} + \epsilon_{\mathrm{A}}(\mathbf{k})\, \hat{n}_{\mathbf{k},\mathrm{A}} \right] + \hat{H}_{\mathrm{AB}}, \tag{16}$$

where $\epsilon_{\mathrm{A}}(\mathbf{k}) = -2t_{\mathrm{A}}[\cos(k_x a) + \cos(k_y a) - 2]$ is the impurity dispersion.

Next, we propose a Chevy-like ansatz [50, 85, 86] for the ground state as

$$|\Psi\rangle = \left[\phi_0 \hat{c}_{\mathbf{k}=0,A}^{\dagger} + \sum_{\mathbf{q}} \phi_{\mathbf{q}} \hat{c}_{\mathbf{q},A}^{\dagger} \hat{\gamma}_{-\mathbf{q}}^{\dagger} \right] |\psi(\theta)\rangle_{\mathrm{BEC}}, \tag{17}$$

with the variational parameters ϕ_0 and $\phi_{\mathbf{q}}$. Note that for $U_{\mathrm{AB}} = 0$, the ground state of the system can be written as

$$|\Phi_0\rangle = \hat{c}^{\dagger}_{\mathbf{k}=0,A}|\psi(\theta)\rangle_{\mathrm{BEC}}, \tag{18}$$

this considers an impurity at the bottom of the band on top of the gas of hard-core bosons. We remark that by construction, the ansatz (17) creates exactly one impurity on top of the BEC. So far, our main approximation is that we consider collective excitations to be bosons. This assumption, which involves considering only the linear terms of the Holstein–Primakoff transformation, implies that the number of perturbations around the ground state in equation (5) is very small. Since our ansatz creates a single excitation of the bath, we retain this approximation. In condensed matter systems, the non-bosonic nature and corrections to the linear regime may lead to intriguing effects [74].

The functions ϕ_0 and $\phi_{\mathbf{q}}$ are obtained from the variational principle $\delta\langle\Psi|\hat{H} - E|\Psi\rangle/\delta\phi_0^* = 0$ and $\delta\langle\Psi|\hat{H} - E|\Psi\rangle/\delta\phi_{\mathbf{p}}^* = 0$, respectively. This ansatz leads to the following set of equations:

$$\epsilon_{\mathrm{MF}}\phi_0 - \frac{U_{\mathrm{AB}}}{2\sqrt{N_s}}\sin\theta\sum_{\mathbf{p}}\phi_{\mathbf{p}}\left(u_{\mathbf{p}} - v_{\mathbf{p}}\right) = E\phi_0, \tag{19a}$$

$$\begin{aligned}&\left[\omega(\mathbf{p}) + \epsilon_A(\mathbf{p}) + \epsilon_{\mathrm{MF}}\right]\phi_{\mathbf{p}} - \frac{U_{\mathrm{AB}}}{2\sqrt{N_s}}\sin\theta\left(u_{\mathbf{p}} - v_{\mathbf{p}}\right)\phi_0\\ &-\frac{1}{N_s}U_{\mathrm{AB}}\cos\theta\sum_{\mathbf{p}'}\left(u_{\mathbf{p}}u_{\mathbf{p}'} + v_{\mathbf{p}}v_{\mathbf{p}'}\right)\phi_{\mathbf{p}'} = E\phi_{\mathbf{p}},\end{aligned} \tag{19b}$$

where $\epsilon_{\mathrm{MF}} = n_{\mathrm{B}}U_{\mathrm{AB}}$ is the mean-field energy.

For the two-dimensional Bose polaron in homogeneous confinement, Chevy's ansatz in [87] has provided a very accurate description compared to quantum Monte Carlo calculations [88], and it is equivalent to the non-self-consistent T-matrix approximation [89]. Furthermore, the limitations of Chevy's ansatz for weakly interacting BEC are related to the formation of clusters around the impurity [13], clusters that, due to the bosonic nature of the atoms forming the BEC, can be arbitrarily large. The formation of large polaron clouds cannot be correctly captured with this ansatz. Here, however, we work in the opposite regime where these clusters are intrinsically prevented due to the hard-core nature of the bosons. Therefore, we expect this ansatz to be even more reliable with the hard-core constraint for the bath bosons.

3. Lattice polarons

We can now investigate the spectral features of the impurity coupled to the hard-core gas and the properties of the resulting lattice polaron. In particular, we perform calculations of the energy, quasiparticle residue and the spectral function. Here, the polaron energy is denoted by E, we shift the energy of the non-interacting impurity and the BEC to zero, such that E, can be read directly as the polaron energy. The quasiparticle residue, Z, is determined by the squared overlap between the interacting $|\Psi\rangle$ and the non-interacting $|\Phi_0\rangle$ states, the latter corresponding to the case where the impurity sits on top of the BEC without creating correlations, see equation (18):

$$Z = |\langle\Phi_0|\Psi\rangle|^2. \tag{20}$$

On the other hand, the spectral function of the impurity is defined by the expression

$$A(\mathbf{k} = 0, \omega) = -\frac{1}{\pi}\mathbf{Im}\left[\sum_{n=0}\frac{|\langle\Phi_0|\Psi_n\rangle|^2}{\omega - E_n + i\eta}\right], \tag{21}$$

where $\{|\Psi_n\rangle\}$ is the set of eigenstates obtained from the diagonalization of equations (19a) and (19b), and E_n denotes the corresponding eigenenergies. For visibility purposes, we add a small imaginary number, $i\eta$, to the spectral function. As we focus on the zero-momentum impurity, we simply denote $A(\mathbf{k} = 0, \omega) = A(\omega)$.

First, we study the zero-momentum polaron energy, E/t, as a function of the angle θ (which varies the filling factor n_{B}) for several values of the interaction strength U_{AB}. This is shown in figure 2, where we show for attractive impurity-boson interactions: $U_{\mathrm{AB}}/t = -10.0$ (red line), $U_{\mathrm{AB}}/t = -5.0$ (blue line), and $U_{\mathrm{AB}}/t = -1.0$ (black line) as well as for repulsive interactions $U_{\mathrm{AB}}/t = 1.0$ (dot-dashed purple line) and $U_{\mathrm{AB}}/t = 5.0$ (dashed orange line). In our numerics, we solve the variational equations by discretizing the first Brillouin zone, in this case, our grid consists of 151×151 points. We take $t_{\mathrm{A}} = t_{\mathrm{B}} = t$.

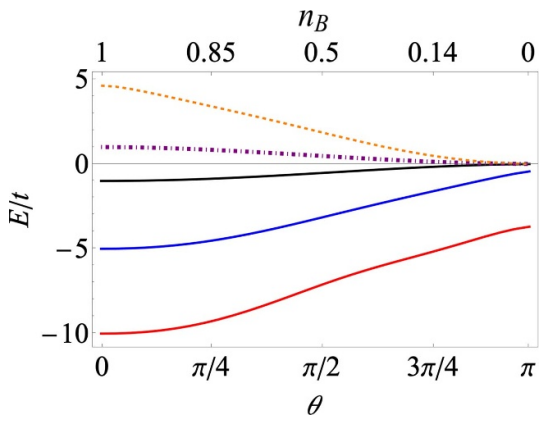

Figure 2. Zero-momentum polaron energies as a function of the angle θ for $U_{AB}/t = -10.0$ (red line), $U_{AB}/t = -5.0$ (blue line), $U_{AB}/t = -1.0$ (black line), $U_{AB}/t = 1.0$ (dot-dashed purple line) and $U_{AB}/t = 5.0$ (dashed orange line). The dependence on the filling factor is depicted at the top of the figure.

For attractive interactions in figure 2, we observe for small angles, i.e. close to unit filling factors, that the polaron energy simply saturates at U_{AB}. Physically, this is very intuitive: when the bosons fill the lattice, there is no longer a continuum of scattering processes, and the energy of adding an impurity is simply given by the energy cost of putting a boson and an impurity together, which is U_{AB}. With increasing angle, that is, decreasing the filling factor, scattering processes start to be allowed, then, the energy of the polaron increases smoothly with the angle θ. Interestingly, we find that when $\theta \to \pi$, that is, $n_B \to 0$, the energy of the polaron does not tend to zero. This is somewhat surprising because in the limit $n_B \to 0$, the problem can be regarded as a B atom placed in an empty lattice, and one would expect that the energy of the polaron to approach zero as $n_B \to 0$. However, this is a partial description and it is not entirely valid in the strong coupling regime. To further understand this unexpected behavior, note that in equation (15), the mean-field and Fröhlich terms of the Hamiltonian vanish when $\theta \to \pi$, while the term beyond Fröhlich remains finite (last three lines in equation (15)). This term increases with U_{AB}, leading to a non-zero polaron energy for $n_B \to 0$. In this limit, both the mean-field and Fröhlich contributions become negligible, and the polaron state is completely dominated by the *beyond Fröhlich* term of the Hamiltonian, this is a genuine result of strong interactions.

The physical explanation for the finite energy of the attractive polaron as the bath density tends to zero can be traced by first considering the opposite regime. Near unit filling, the energy of the polaron is $E \sim U_{AB}$, which simply represents the energy of double occupation where the impurity and a lattice boson occupy the same site. Since the lattice is filled, this is the only state available. As we decrease the filling factor, scattering states become available, and the impurity can occupy empty sites, but it can also occupy a filled state and move as a dimer with a boson of the BEC, forming a two-body bound state. For strong interactions, the dimer state becomes robust and persists at small densities of the BEC; this represents a true two-body bound state with a non-zero binding energy for $n_B \to 0$. Then, we would expect the energy of the polaron to lie below the energy of the bound state. Confined to optical lattices, the study of the scattering between a pair of atoms from a two-body perspective [90–92] has predicted the emergence of both long-lived attractive and repulsive bound states, which were experimentally observed [93].

For repulsive interactions, we observe that close to unit filling ($\theta = 0$), the energy of the polaron saturates to $E \sim U_{AB}$, as shown in figure 2. With increasing angle (decreasing filling factor), the polaron energy smoothly decreases and tends to zero as the filling factor approaches zero. Our findings suggest that for strong coupling, the repulsive and attractive polaron behave differently in the limit $n_B \to 0$.

To understand the quasiparticle character of the polaron states discussed above, we now turn to the polaron residue as defined in equation (20). In figure 3, we show the residue Z as a function of the angle θ and the interaction strength U_{AB}/t. For weak attractive interactions, we find that the polaron is well-defined with $Z \sim 1$. As the interaction strength increases, the polaron remains a well-defined quasiparticle only for small angles (close to unit filling factors). In contrast, for small filling factors ($\theta \to \pi$), the residue of the polaron starts dropping to zero. That is, the states we discussed previously, where the energy of the ground-state remains non-zero in the limit $n_B \to 0$, have indeed very small residue and are consequently ill-defined quasiparticles. Note that in this same limit ($n_B \to 0$), the residue of the repulsive polaron is close to one, meaning that in this case, this branch remains as a well-defined quasiparticle. On the other hand, close to unit filling and for strong coupling, the repulsive polaron cedes its spectral weight and is no longer a well-defined quasiparticle. Thus, we obtain opposite behaviors for attractive and repulsive polarons: For

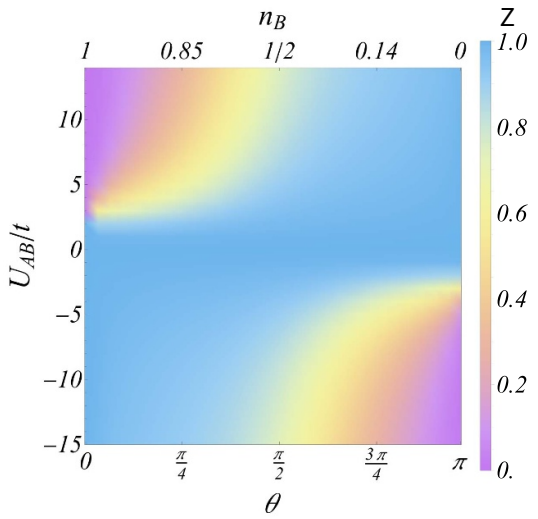

Figure 3. Quasiparticle residue, Z, for the zero-momentum polaron as a function of the interaction strength, U_{AB}, and the angle θ which determines the filling factor (see top).

strong interactions, we have found that the low-energy polaron state becomes ill-defined as n_{B} approaches 0 for attractive interactions and as n_{B} approaches 1 for repulsive interactions. Furthermore, the residue in figure 3 exhibits symmetry under $(\theta, U_{\mathrm{AB}}) \to (\theta - \pi, -U_{\mathrm{AB}})$, highlighting a particle-hole symmetry. This symmetry implies that scattering processes can be understood in terms of the interactions of an impurity with either a particle or a hole.

One should remark that the breakdown of the quasiparticle picture occurs only for strong interactions. For weak impurity-boson interactions, we obtain that the quasiparticle picture holds valid for all filling factors, including the limit cases of $n_{\mathrm{B}} \to 0$ and $n_{\mathrm{B}} \to 1$.

Now, we can complete the physical picture of the intriguing behavior of the attractive polaron energy at low densities based on the residue observations. Attractive strong interactions allow the binding of the impurity and a boson of the bath; the energy of the dimer state is below zero and sets an upper bound on the polaron energy. As the density of the bath decreases, the residue of the attractive polaron branch also decreases. Physically, this can be understood by the fact that as the density decreases, the impurity finds fewer bosonic atoms to bind with. Therefore, this state becomes less accessible, leading to a vanishing residue.

Since our approach preserves the sum-rule $\int A(\omega)\mathrm{d}\omega = 1$, if the polaron loses its residue, the spectral weight has to be distributed in high-energy excitations. Physically, these states can be understood as a continuum of scattering states formed by an impurity state with finite momentum $\mathbf{k}$ and a collective excitation of the BEC, $\hat{\gamma}^{\dagger}_{-\mathbf{k}}$, with opposite momentum $\mathbf{k}$. Indeed, our variational ansatz provides not only the residue of the polaron, $\phi_0 = \sqrt{Z}$, but also the weight of these scattering states, $\phi_{\mathbf{k}}$.

To understand how the spectral weight is transferred into high-energy excitations, we plot in figure 4 the spectral function, $A(\omega)$, as a function of the frequency ω/t for fixed $U_{\mathrm{AB}}/t = -5$ and several filling factor values.

Figure 4 shows the evolution of the polaron peak with decreasing density (increasing θ) for strong impurity-boson interactions. For large filling factors (small angles), the polaron peak retains most of the spectral weight, as shown by the red line in figure 4; in this case, only the quasiparticle peak at $\omega/t \approx U_{\mathrm{AB}}/t = -5$ is visible in the spectral function. By decreasing the filling factor (increasing θ), we observe a reduction of polaron peak, as indicated by the blue and black curves for $\theta = 3\pi/4$ and $\theta = 7\pi/8$, respectively. As the polaron peak shrinks, its spectral weight is transferred into high-energy excitations, these excitations are incoherent and consist of the continuum of excitations of our ansatz in equation (17); i.e. this continuum is formed by one collective excitation of the BEC and an impurity state with opposite momentum. Close to $\theta = \pi$, the polaron peak has disappeared and the quasiparticle residue vanishes, distributing its spectral weight in the continuum of excitations which become more visible (purple line).

Due to the confinement of the BEC and the impurity within an optical lattice, the continuum of excitations is bounded from above and below. The width is given by $W = 4t[2 + \sqrt{2(1 + \cos^2\theta)}]$, which depends on θ. Note that the fading of the polaron in the strong coupling regime is a result that only the beyond Fröhlich term in the Hamiltonian of equation (15) can capture.

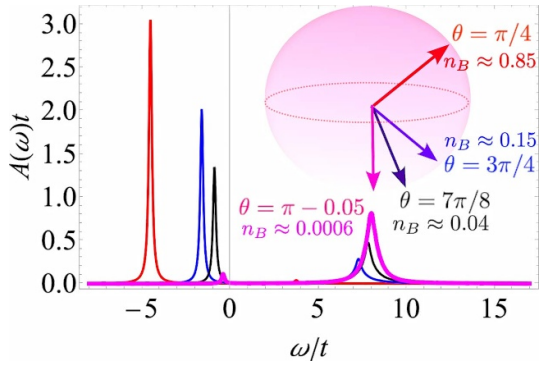

Figure 4. Spectral function, $A(\omega)$, as a function of the frequency ω/t with $U_{AB}/t = -5$ for $\theta = \pi/4$ (red line), $\theta = 3\pi/4$ (blue line), $\theta = 7\pi/8$ (black line) and $\theta = \pi - 0.05$ (purple line). With increasing angle (decreasing the filling factor), we observe that the polaron becomes ill-defined and cedes its spectral weight to the continuum of collective excitations.

4. Discussion and conclusions

In this work, we have studied the problem of an impurity coupled to a BEC of hard-core bosons in a two-dimensional optical lattice. Employing a variational ansatz to describe the formation of the Bose polaron for strong coupling, we unveiled the quasiparticle properties of the zero-momentum impurity and have shown the interplay between the strong impurity-boson interactions and the inherent collective excitations of the hard-core bosons which tune the quasiparticle features.

As mentioned, the study of the strongly interacting Bose polaron in homogeneous or harmonic confinements, that is, without the lattice, has attracted significant attention. Therefore, it is important to discuss the aspects that are genuine lattice polaron features. Experimentally, the first observations of attractive and repulsive polarons unveiled an interplay between these quasiparticle branches [32, 33]. These polaron states also emerge in lattice confinement. One of the most notable differences between homogeneous and lattice polarons is the nature of the continuum of scattering states. While unbound for homogeneous polarons, in a lattice, these states are bounded both from above and below, which changes the underlying character of the quasiparticle and can give rise to the emergence of repulsive bound states.

On the other hand, many aspects of the lattice polaron in a condensate of hard-core bosons remain to be studied, aspects that for homogeneous Bose polarons have unveiled many intriguing properties. These include non-equilibrium dynamics [37, 38], criticality [35], and universal properties [39]. All these motivate further theoretical and numerical developments to understand lattice hard-core polarons beyond the Chevy ansatz-like approach. Due to the reduced dimensionality of the system, approaches such as exact diagonalization [52], quantum Monte Carlo, DMRG, or other sophisticated many-body techniques [94] may be suitable for studying these kinds of systems. Furthermore, an interesting avenue is to study the Fermi lattice polaron, which may reveal new physics such as the polaron-to-molecule crossover in a lattice, a phenomenon extensively studied in homogeneous confinements [95–98].

The ability to probe lattice systems site-by-site using quantum microscopy has increased interest in the study of lattice polarons, which may serve as probes to measure quantum phase transitions [40], topological and geometric features [41–44], as well as following spatially non-equilibrium dynamics [51]. Entering into the strongly interacting regime may lead to the emergence of new few-body and many-body states [50].

In ultracold gases, the breakthrough experimental progress to realize binary mixtures confined in optical lattices make our proposal realistic. For instance, a population-imbalanced Bose–Fermi mixture can be produced with bosonic ^{87}Rb and fermionic ^{40}K. This mixture is attractive in view of the existing Feshbach resonance between the Rubidium and Potassium atoms, allowing for tuning the impurity-boson interactions on demand.

Van der Waals heterostructures have opened new avenues for realizing strongly correlated phases in periodically confined systems. In bilayers, moiré superlattices enable the realization of Hubbard models [80, 81]. Very recently, the first Bose–Fermi–Hubbard model was realized in these systems [82]. Given the ability to tune Hubbard model parameters through the relative twist angle, we expect our study to draw attention towards realizing mediated superconductivity in these systems.

Data availability statement

The data that support the findings of this study are openly available at the following URL/DOI: https://doi.org/10.5281/zenodo.10841578.

Acknowledgment

We thank David Ruiz-Tijerina for valuable discussions and comments to our manuscript. M S G acknowledges to Consejo Nacional de Humanidades, Ciencias y Tecnología (CONAHCYT) for the scholarship provided. A C G acknowledges financial support from UNAM DGAPA PAPIIT Grant No. IA101923, and UNAM DGAPA PAPIME Grants Nos. PE101223 and PIIF23. S G C L acknowledges financial support from UNAM DGAPA PAPIIT Grant No. TA100724.

References

[1] Bloch I, Dalibard J and Nascimbene S 2012 Quantum simulations with ultracold quantum gases *Nat. Phys.* **8** 267–76
[2] Georgescu I M, Ashhab S and Nori F 2014 Quantum simulation *Rev. Mod. Phys.* **86** 153–85
[3] Gross C and Bloch I 2017 Quantum simulations with ultracold atoms in optical lattices *Science* **357** 995–1001
[4] Schäfer F, Fukuhara T, Sugawa S, Takasu Y and Takahashi Y 2020 Tools for quantum simulation with ultracold atoms in optical lattices *Nat. Rev. Phys.* **2** 411–25
[5] Greiner M, Mandel O, Esslinger T, Hänsch T W and Bloch I 2002 Quantum phase transition from a superfluid to a mott insulator in a gas of ultracold atoms *Nature* **415** 39–44
[6] Tarruell L and Sanchez-Palencia L 2018 Quantum simulation of the hubbard model with ultracold fermions in optical lattices *C. R. Physique* **19** 365–93
[7] Rath S P and Schmidt R 2013 Field-theoretical study of the Bose polaron *Phys. Rev.* A **88** 053632
[8] Ardila L A P na and Giorgini S 2015 Impurity in a Bose-Einstein condensate: Study of the attractive and repulsive branch using quantum Monte Carlo methods *Phys. Rev.* A **92** 033612
[9] Shchadilova Y E, Schmidt R, Grusdt F and Demler E 2016 Quantum dynamics of ultracold Bose polarons *Phys. Rev. Lett.* **117** 113002
[10] Grusdt F, Seetharam K, Shchadilova Y and Demler E 2018 Strong-coupling Bose polarons out of equilibrium: dynamical renormalization-group approach *Phys. Rev.* A **97** 033612
[11] Christensen R S, Levinsen J and Bruun G M 2015 Quasiparticle properties of a mobile impurity in a Bose-Einstein condensate *Phys. Rev. Lett.* **115** 160401
[12] Christianen A, Cirac J I and Schmidt R 2024 Phase diagram for strong-coupling Bose polarons *SciPost Phys.* **16** 067
[13] Levinsen J, Ardila L A P na, Yoshida S M and Parish M M 2021 Quantum behavior of a heavy impurity strongly coupled to a Bose gas *Phys. Rev. Lett.* **127** 033401
[14] Levinsen J, Parish M M and Bruun G M 2015 Impurity in a Bose-Einstein condensate and the Efimov effect *Phys. Rev. Lett.* **115** 125302
[15] Sun M, Zhai H and Cui X 2017 Visualizing the Efimov correlation in Bose polarons *Phys. Rev. Lett.* **119** 013401
[16] Sun M and Cui X 2017 Enhancing the Efimov correlation in Bose polarons with large mass imbalance *Phys. Rev.* A **96** 022707
[17] Christianen A, Cirac J I and Schmidt R 2022 Chemistry of a light impurity in a Bose-Einstein condensate *Phys. Rev. Lett.* **128** 183401
[18] Christianen A, Cirac J I and Schmidt R 2022 Bose polaron and the Efimov effect: a Gaussian-state approach *Phys. Rev.* A **105** 053302
[19] Yoshida S M, Endo S, Levinsen J and Parish M M 2018 Universality of an impurity in a Bose-Einstein condensate *Phys. Rev.* X **8** 011024
[20] Massignan P, Yegovtsev N and Gurarie V 2021 Universal aspects of a strongly interacting impurity in a dilute Bose condensate *Phys. Rev. Lett.* **126** 123403
[21] Yegovtsev N, Massignan P and Gurarie V 2022 Strongly interacting impurities in a dilute Bose condensate *Phys. Rev.* A **106** 033305
[22] Skou M G, Skov T G, Jørgensen N B and Arlt J J 2021 Initial dynamics of quantum impurities in a Bose-Einstein condensate *Atoms* **9** 22
[23] Cayla H, Massignan P, Giamarchi T, Aspect A, Westbrook C I and Clément D 2023 Observation of 1/k 4-tails after expansion of Bose-Einstein condensates with impurities *Phys. Rev. Lett.* **130** 153401
[24] Nielsen K K and Ardila L A P na 2019 Critical slowdown of non-equilibrium polaron dynamics *New J. Phys.* **21** 043014
[25] Guenther N-E, Schmidt R, Bruun G M, Gurarie V and Massignan P 2021 Mobile impurity in a Bose-Einstein condensate and the orthogonality catastrophe *Phys. Rev.* A **103** 013317
[26] Bighin G, Burchianti A, Minardi F and Macri T 2022 Impurity in a heteronuclear two-component Bose mixture *Phys. Rev.* A **106** 023301
[27] Camacho-Guardian A 2023 Polaritons for testing the universality of an impurity in a Bose-Einstein condensate *Phys. Rev.* A **108** L021303
[28] Liu N 2024 Weak and strong coupling polarons in binary Bose-Einstein condensates (arXiv:2401.11808 [cond-mat.quant-gas])
[29] Isaule F 2024 Functional renormalisation group approach to the finite-temperature Bose polaron (arXiv:2402.04197)
[30] Seetharam K, Shchadilova Y, Grusdt F, Zvonarev M B and Demler E 2021 Dynamical quantum Cherenkov transition of fast impurities in quantum liquids *Phys. Rev. Lett.* **127**
[31] Seetharam K, Shchadilova Y, Grusdt F, Zvonarev M and Demler E 2021 Quantum Cherenkov transition of finite momentum Bose polarons (arXiv:2109.12260)
[32] Jørgensen N B, Wacker L, Skalmstang K T, Parish M M, Levinsen J, Christensen R S, Bruun G M and Arlt J J 2016 Observation of attractive and repulsive polarons in a Bose-Einstein condensate *Phys. Rev. Lett.* **117** 055302
[33] Hu M-G, Van de Graaff M J, Kedar D, Corson J P, Cornell E A and Jin D S 2016 Bose polarons in the strongly interacting regime *Phys. Rev. Lett.* **117** 055301

[34] Ardila L A P na, Jørgensen N B, Pohl T, Giorgini S, Bruun G M and Arlt J J 2019 Analyzing a Bose polaron across resonant interactions *Phys. Rev.* A **99** 063607
[35] Yan Z Z, Ni Y, Robens C and Zwierlein M W 2020 Bose polarons near quantum criticality *Science* **368** 190–4
[36] Skou M G, Skov T G, Jørgensen N B, Nielsen K K, Camacho-Guardian A, Pohl T, Bruun G M and Arlt J J 2021 Non-equilibrium quantum dynamics and formation of the Bose polaron *Nat. Phys.* **17** 731–5
[37] Skou M G, Nielsen K K, Skov T G, Morgen A M, Jørgensen N B, Camacho- Guardian A, Pohl T, Bruun G M and Arlt J J 2022 Life and death of the Bose polaron *Phys. Rev. Res.* **4** 043093
[38] Morgen A M, Balling S S, Nielsen K K, Pohl T, Bruun G M and Arlt J J 2023 Quantum beat spectroscopy of repulsive Bose polarons (arXiv:2310.18183)
[39] Etrych J, Martirosyan G, Cao A, Ho C J, Hadzibabic Z and Eigen C 2024 Universal quantum dynamics of Bose polarons (arXiv:2402.14816)
[40] Colussi V E, Caleffi F, Menotti C and Recati A 2023 Lattice polarons across the superfluid to mott insulator transition *Phys. Rev. Lett.* **130** 173002
[41] Grusdt F, Yao N Y, Abanin D, Fleischhauer M and Demler E 2016 Interferometric measurements of many-body topological invariants using mobile impurities *Nat. Commun.* **7** 11994
[42] Camacho-Guardian A, Goldman N, Massignan P and Bruun G M 2019 Dropping an impurity into a chern insulator: a polaron view on topological matter *Phys. Rev.* B **99** 081105
[43] Pimenov D, Camacho-Guardian A, Goldman N, Massignan P, Bruun G M and Goldstein M 2021 Topological transport of mobile impurities *Phys. Rev.* B **103** 245106
[44] Pimenov D 2024 Polaron spectra and edge singularities for correlated flat bands *Phys. Rev.* B **109** 195153
[45] Koepsell J *et al* 2021 Microscopic evolution of doped mott insulators from polaronic metal to fermi liquid *Science* **374** 82–86
[46] Grusdt F, Kánasz-Nagy M, Bohrdt A, Chiu C S, Ji G, Greiner M, Greif D and Demler E 2018 Parton theory of magnetic polarons: mesonic resonances and signatures in dynamics *Phys. Rev.* X **8** 011046
[47] Wang Y, Bohrdt A, Ding S, Koepsell J, Demler E and Grusdt F 2021 Higher-order spin-hole correlations around a localized charge impurity *Phys. Rev. Res.* **3** 033204
[48] Nielsen K K, Bastarrachea-Magnani M A, Pohl T and Bruun G M 2021 Spatial structure of magnetic polarons in strongly interacting antiferromagnets *Phys. Rev.* B **104** 155136
[49] Nielsen K K 2022 Exact nonequilibrium hole dynamics, magnetic polarons and string excitations in antiferromagnetic bethe lattices *Phys. Rev.* B **106** 115144
[50] Ding S, Domínguez-Castro G A, Julku A, Camacho-Guardian A and Bruun G M 2023 Polarons and bipolarons in a two-dimensional square lattice *SciPost Phys.* **14** 143
[51] Isaule F, Rojo-Francas A and Juliá-Díaz B 2024 Bound impurities in a one-dimensional Bose lattice gas: low-energy properties and quench-induced dynamics (arXiv:2402.03070)
[52] Amelio I and Goldman N 2024 Polaron spectroscopy of interacting fermi systems: insights from exact diagonalization *SciPost Phys.* **16** 056
[53] Bakr W S, Gillen J I, Peng A, Fölling S and Greiner M 2009 A quantum gas microscope for detecting single atoms in a hubbard-regime optical lattice *Nature* **462** 74–77
[54] Bakr W S, Peng A, Tai M E, Ma R, Simon J, Gillen J I, Foelling S, Pollet L and Greiner M 2010 Probing the superfluid–to–mott insulator transition at the single-atom level *Science* **329** 547–50
[55] Hilker T A, Salomon G, Grusdt F, Omran A, Boll M, Demler E, Bloch I and Gross C 2017 Revealing hidden antiferromagnetic correlations in doped hubbard chains via string correlators *Science* **357** 484–7
[56] Takemura N, Trebaol S, Wouters M, Portella-Oberli M T and Deveaud Bit 2014 Polaritonic feshbach resonance *Nat. Phys.* **10** 500–4
[57] Takemura N, Anderson M D, Navadeh-Toupchi M, Oberli D Y, Portella-Oberli M T and Deveaud B 2017 Spin anisotropic interactions of lower polaritons in the vicinity of polaritonic feshbach resonance *Phys. Rev.* B **95** 205303
[58] Navadeh-Toupchi M, Takemura N, Anderson M D, Oberli D Y and Portella-Oberli M T 2019 Polaritonic cross feshbach resonance *Phys. Rev. Lett.* **122** 047402
[59] Tan Li B, Diessel O K, Popert A, Schmidt R, Imamoglu A and Kroner M 2023 Bose polaron interactions in a cavity-coupled monolayer semiconductor *Phys. Rev.* X **13** 031036
[60] Wasak T, Schmidt R and Piazza F 2021 Quantum-zeno fermi polaron in the strong dissipation limit *Phys. Rev. Res.* **3** 013086
[61] Vashisht A, Richard M and Minguzzi A 2022 Bose polaron in a quantum fluid of light *SciPost Phys.* **12** 008
[62] Bastarrachea-Magnani M A, Camacho-Guardian A, Wouters M and Bruun G M 2019 Strong interactions and biexcitons in a polariton mixture *Phys. Rev.* B **100** 195301
[63] Camacho-Guardian A, Bastarrachea-Magnani M A and Bruun G M 2021 Mediated interactions and photon bound states in an exciton-polariton mixture *Phys. Rev. Lett.* **126** 017401
[64] Levinsen J, Marchetti F M, Keeling J and Parish M M 2019 Spectroscopic signatures of quantum many-body correlations in polariton microcavities *Phys. Rev. Lett.* **123** 266401
[65] Ruiz-Tijerina D A 2023 Bose–fermi mixtures in 2D solid-state superstructures *Nat. Mater.* **22** 153–4
[66] Shimazaki Y, Kuhlenkamp C, Schwartz I, Smoleński T, Watanabe K, Taniguchi T, Kroner M, Schmidt R, Knap M and Imamoğlu A 2021 Optical signatures of periodic charge distribution in a mott-like correlated insulator state *Phys. Rev.* X **11** 021027
[67] Smoleński T *et al* 2021 Signatures of wigner crystal of electrons in a monolayer semiconductor *Nature* **595** 53–57
[68] Mazza G and Amaricci A 2022 Strongly correlated exciton-polarons in twisted homobilayer heterostructures *Phys. Rev.* B **106** L241104
[69] Amelio I, Drummond N D, Demler E, Schmidt R and Imamoglu A 2023 Polaron spectroscopy of a bilayer excitonic insulator *Phys. Rev.* B **107** 155303
[70] Julku A, Ding S, and Bruun G M 2023 An exciton interacting with a moire lattice–polarons, strings, and optical probing of spin correlations (arXiv:2311.03482)
[71] Kennes D M, Claassen M, Xian L, Georges A, Millis A J, Hone J, Dean C R, Basov D N, Pasupathy A N and Rubio A 2021 Moiré heterostructures as a condensed-matter quantum simulator *Nat. Phys.* **17** 155–63
[72] Huang Di, Choi J, Shih C-K and Li X 2022 Excitons in semiconductor moiré superlattices *Nat. Nanotechnol.* **17** 227–38
[73] Tang Y *et al* 2020 Simulation of hubbard model physics in WSe_2/Ws_2 Moiré superlattices *Nature* **579** 353–8
[74] Huang T-S, Lunts P and Hafezi M 2024 Nonbosonic moiré excitons *Phys. Rev. Lett.* **132** 186202
[75] Remez B and Cooper N R 2022 Leaky exciton condensates in transition metal dichalcogenide Moiré bilayers *Phys. Rev. Res.* **4** L022042

[76] Julku A 2022 Nonlocal interactions and supersolidity of Moiré excitons *Phys. Rev.* B **106** 035406
[77] Ospelkaus S, Ospelkaus C, Wille O, Succo M, Ernst P, Sengstock K and Bongs K 2006 Localization of bosonic atoms by fermionic impurities in a three-dimensional optical lattice *Phys. Rev. Lett.* **96** 180403
[78] Günter K, Stöferle T, Moritz H, Köhl M and Esslinger T 2006 Bose-fermi mixtures in a three-dimensional optical lattice *Phys. Rev. Lett.* **96** 180402
[79] Best T, Will S, Schneider U, Hackermüller L, van Oosten D, Bloch I and Lühmann D-S 2009 Role of interactions in ^{87}Rb–^{40}**K** Bose-Fermi mixtures in a 3D optical lattice *Phys. Rev. Lett.* **102** 030408
[80] Schuster T, Scelle R, Trautmann A, Knoop S, Oberthaler M K, Haverhals M M, Goosen M R, Kokkelmans S J J M F and Tiemann E 2012 Feshbach spectroscopy and scattering properties of ultracold Li^+ Na mixtures *Phys. Rev.* A **85** 042721
[81] Bernardet K, Batrouni G G, Meunier J-L, Schmid G, Troyer M and Dorneich A 2002 Analytical and numerical study of hardcore bosons in two dimensions *Phys. Rev.* B **65** 104519
[82] Santiago-García M and Camacho-Guardian A 2023 Collective excitations of a Bose–Einstein condensate of hard-core bosons and their mediated interactions: from two-body bound states to mediated superfluidity *New J. Phys.* **25** 093032
[83] Boninsegni M and Prokof'ev N 2005 Supersolid phase of hard-core bosons on a triangular lattice *Phys. Rev. Lett.* **95** 237204
[84] Prabhakar A and Stancil D D 2009 *Spin Waves: Theory and Applications* vol 5 (Springer)
[85] Chevy F 2006 universal phase diagram of a strongly interacting fermi gas with unbalanced spin populations *Phys. Rev.* A **74** 063628
[86] Li W and Das Sarma S 2014 Variational study of polarons in Bose-Einstein condensates *Phys. Rev.* A **90** 013618
[87] Nakano Y, Parish M M and Levinsen J 2024 Variational approach to the two-dimensional Bose polaron *Phys. Rev.* A **109** 013325
[88] Ardila L A P na, Astrakharchik G E and Giorgini S 2020 Strong coupling Bose polarons in a two-dimensional gas *Phys. Rev. Res.* **2** 023405
[89] Cárdenas-Castillo L F and Camacho-Guardian A 2022 Strongly interacting Bose polarons in two-dimensional atomic gases and quantum fluids of polaritons *Atoms* **11** 3
[90] Piil R and Mølmer K 2007 Tunneling couplings in discrete lattices, single-particle band structure and eigenstates of interacting atom pairs *Phys. Rev.* A **76** 023607
[91] Valiente M and Petrosyan D 2008 Two-particle states in the hubbard model *J. Phys. B: At. Mol. Opt. Phys.* **41** 161002
[92] Camacho-Guardian A, Domínguez-Castro G A and Paredes R 2016 Bound states and cooper pairs of molecules in 2D optical lattices bilayer *Ann. Phys., Lpz.* **528** 580–7
[93] Winkler K, Thalhammer G, Lang F, Grimm R, Hecker Denschlag J, Daley A J, Kantian A, Büchler H P and Zoller P 2006 Repulsively bound atom pairs in an optical lattice *Nature* **441** 853–6
[94] Zhao Y 2023 The hierarchy of davydov's ansätze: from guesswork to numerically "exact" many-body wave functions *J. Chem. Phys.* **158** 080901
[95] Punk M, Dumitrescu P T and Zwerger W 2009 Polaron-to-molecule transition in a strongly imbalanced fermi gas *Phys. Rev.* A **80** 053605
[96] Massignan P, Zaccanti M and Bruun G M 2014 Polarons, dressed molecules and itinerant ferromagnetism in ultracold fermi gases *Rep. Prog. Phys.* **77** 034401
[97] Parish M M 2011 Polaron-molecule transitions in a two-dimensional fermi gas *Phys. Rev.* A **83** 051603
[98] Ness G, Shkedrov C, Florshaim Y, Diessel O K, von Milczewski J, Schmidt R and Sagi Y 2020 Observation of a smooth polaron-molecule transition in a degenerate fermi gas *Phys. Rev.* X **10** 041019